The B 1 Σ + and X 1 Σ + Electronic States of Hydrogen Fluoride: A Direct Potential Fit Analysis

2 **AUTHORS**, INCLUDING:

Photos Hajigeorgiou

University of Nicosia

36 PUBLICATIONS   **792** CITATIONS

The *B* ¹Σ⁺ and *X* ¹Σ⁺ Electronic States of Hydrogen Fluoride: A Direct Potential Fit Analysis

John A. Coxon*

Department of Chemistry, Dalhousie University, Halifax, Nova Scotia, Canada B3H 4J3

Photos G. Hajigeorgiou

Department of Life and Health Sciences, Intercollege, 46 Makedonitissas Avenue, P.O. Box 24005, 1700 Nicosia, Cyprus

All literature pure rotational and vibration−rotational spectroscopic data on the ground $X\,^1\Sigma^+$ electronic state of HF and DF, together with the entire set of spectroscopic line positions from analyses of the $B\,^1\Sigma^+ \rightarrow X\,^1\Sigma^+$ emission band systems of HF and DF, have been used in a global least-squares fit to the radial Hamiltonian operators, in compact analytic form, for both electronic states. With a data set consisting of 6157 spectroscopic line positions, the reduced standard deviation of the fit was $\hat{\sigma} = 1.028$. Sets of quantum mechanically significant rotational and centrifugal distortion constants were calculated for both electronic states using Rayleigh−Schrödinger perturbation theory.

I. Introduction

In recent years, an increasingly common practice in the literature of diatomic molecule spectroscopy is the representation of measured line positions in terms of the quantum mechanical eigenvalues of vibration−rotational Hamiltonian functions. Some impetus to the development of this methodology on a wider basis was provided by our analysis of the spectroscopic database for the $X\,^1\Sigma^+$ ground electronic states of the hydrogen halides HI and HBr.[1] Although the principal objective of that work was the characterization of Born−Oppenheimer breakdown (BOB) effects in diatomic hydrides, a new and important feature was the introduction of a compact and flexible analytical model for the internuclear potential energy function. Analogous investigations for HF[2] and HCl[3] had been carried out prior to the introduction of empirical analytical models in the procedure, and the potential energy functions in those studies were reported as extensive numerical listings. This was considered a significant drawback and likely dissuaded other investigators from employing the results in related work.

With further refinement of the procedure employing analytical potential functions, a new analysis was performed recently[4] for the spectroscopic data available for the four most abundant isotopologues of HCl. Aside from the novelty of including analytical models, we simultaneously included more recently obtained spectroscopic line positions. This allowed us to report the most precise to date Hamiltonian operators for the $X\,^1\Sigma^+$ and $B\,^1\Sigma^+$ electronic states in compact analytical form.

The present work represents an analogous extension of the previous study on HF,[2] whereby new accurate HF and DF spectroscopic data are included, and the various determinable radial functions are now reported exclusively in analytical form.

The vibration−rotation bands of HF were among the earliest molecular transitions to be studied by infrared absorption

* Corresponding author. Tel: (902) 494-3716. Fax: (902) 494-1310. E-mail: John.Coxon@Dal.Ca.

spectroscopy.[5,6] After more than 80 years, the same transitions are still being studied, but with ever increasing precision of measurement. Also more recently, the same transitions in emission have led to the use of HF gas as the medium of a valuable chemical laser. Moreover, HF has gained astrophysical importance: the detection in 1997 of trace amounts of hydrogen fluoride in the Sagittarius B2 interstellar gas cloud constituted the first discovery of a fluorine-containing molecule in interstellar space.[7]

With such extensive laboratory investigations of the ground $X\,^1\Sigma^+$ electronic state of HF, which also now include studies of pure rotational transitions, it comes as no surprise that numerous complementary ab initio studies have also been undertaken. However, even the most recent calculations[8−10] fail to reproduce the full manifold of vibrational energy levels of the X state with close to spectroscopic accuracy; on average the magnitude of the differences between observed and theoretically calculated vibrational energies is typically ∼80 cm⁻¹. However, although limited to relatively low vibrational levels, the somewhat earlier calculations of Martin[11] were much more successful in predicting the observed vibrational intervals of HF and several other diatomics. In the case of HF(*X*), the first five intervals were calculated to within ∼0.2 cm⁻¹. Other theoretical work has been undertaken to facilitate assignments of complex experimental spectra in the ultraviolet region, involving perturbed Rydberg electronic states. The comprehensive ab initio study of Bettendorff et al.,[12] for example, provided convincing interpretations of the ultraviolet absorption spectra of Douglas and Greening.[13] The theoretical work also offered a lucid explanation for the high degree (∼41%) of ionic character in the $X\,^1\Sigma^+$ state, as also indicated by the large dipole moment (1.83 D). This was shown to arise from a strongly avoided crossing with the $B\,^1\Sigma^+$ state, where the nonadiabatic coupling matrix element $\langle X\,^1\Sigma^+ | \partial/\partial R | B\,^1\Sigma^+ \rangle$ reaches its maximum strength near 3.5 bohr.[12] The bonding character of the ground state changes from ionic $1\sigma^2\,2\sigma^2\,3\sigma^2\,1\pi^4$ to valence
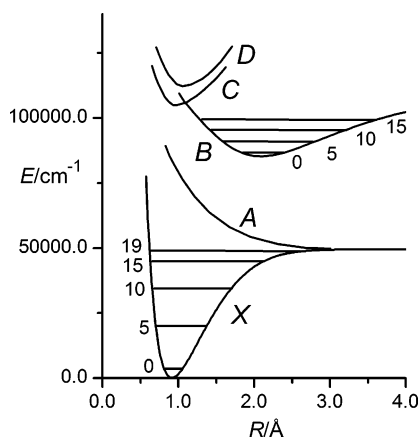
Figure 1. Potential energy curves for selected low-lying electronic states of HF.

$1\sigma^2\ 2\sigma^2\ 3\sigma^1\ 1\pi^4\ 4\sigma^1$ with increasing internuclear separation, furnishing $H(^2S) + F(^2P)$ dissociation products, while the $B\ ^1\Sigma^+$ state, which dissociates to $H^+ + F^-(^1S)$, follows a complementary opposite trend. Figure 1 shows selected electronic states of HF.

Hydrogen fluoride is a light molecule and it is well-known that the Born–Oppenheimer approximation fails to provide an accurate description of this system. At the level of the adiabatic approximation, different effective potentials are predicted for the two isotopologues, HF and DF. In addition to the adiabatic corrections, the low-lying and predominantly repulsive $1\sigma^2\ 2\sigma^2\ 3\sigma^2\ 1\pi^3\ 4\sigma^1 - A\ ^1\Pi$ electronic state, which dissociates to the same limit as the X state (see Figure 1), is responsible for smooth but increasingly severe heterogeneous nonadiabatic perturbations of the rotational energy level manifold of the ground state. In previous work,[2] we achieved a deperturbation of the ground state from such effects by including a radial function $q(R)$ in the centrifugal term of the Hamiltonian operator for the X state. The first identification of such smooth global J-dependent effects in the spectra of diatomic molecules was made by Coxon[14] for the analogous system of hydrogen chloride, in work that laid the foundation for the proper treatment of hydride diatomic spectra by numerical methodology. In subsequent work, Coxon and Hajigeorgiou[2] investigated the isotopic dependence of BOB effects in HF and DF employing a method similar to inverse perturbation analysis (IPA)[15,16] and obtained the potential energy functions for the X and B states, albeit in numerical form on a radial grid. Because a prominent drawback of this methodology was the lack of compactness in the associated functions, we also presented more useful RKR-style listings for the $X\ ^1\Sigma^+$ and $B\ ^1\Sigma^+$ state potentials of HF and DF.[2]

This problem has now been overcome by incorporating analytical models in the procedure, converting the method from IPA to an iterative direct potential fit (DPF) method. A highly successful empirical model for the potential energy of a diatomic molecule is the modified Lennard-Jones (MLJ) oscillator of Hajigeorgiou and Le Roy.[17] This analytical model has been employed successfully in the analysis of HCl data,[4] and for other diatomic molecules, such as CO,[18] HeH$^+$,[19] and LiH.[20] Its most challenging application to date, however, concerns the recent analysis of Li$_2$ data by Coxon and Melville,[21] where data for the $A\ ^1\Sigma^+$ state extend to $R \approx 55$ Å, far beyond the Le Roy radius,[22] a quantity that approximates the internuclear separation associated with the onset of the long-range region.

Other research groups have also employed the DPF method in the early stages of its development in achieving compact representations of large spectroscopic data sets, and we find it

constructive to include a short review of these contributions. Gruebele et al.[23] applied an analytical potential model to represent the spectroscopic transitions of the cations OH$^+$ and ArH$^+$, including a consideration of adiabatic and nonadiabatic corrections. Tiemann[24] applied the DPF method in representing excited electronic state potential functions having an attractive limb potential barrier, for TlF($B\ ^3\Pi_1$), InCl($C\ ^1\Pi$), AlBr($C\ ^1\Pi$), and Na$_2$($B\ ^1\Pi_u$). Brühl et al.[25] also employed the DPF method in the representation by analytic models of the $A\ ^2\Pi$ and $X\ ^2\Sigma^+$ electronic state potentials of the van der Waals molecule NaKr, which was especially challenging owing to the unusually shallow potentials, having well depths of less than 800 cm^{-1}, and supporting few vibrational levels. Significant contributions in the development and refinement of the DPF method have also been made by the Bernath group.[26-28] In recent years there have been new applications of the DPF methodology, which are far too numerous to note here, but the increasing frequency of these applications is encouraging because it clearly indicates the wider establishment of the method.

The present work incorporates an application of the DPF procedure to the large spectroscopic database containing all available HF/DF ($X\ ^1\Sigma^+$) pure-rotational and vibration–rotational transitions, as well as the rotationally hot $B\ ^1\Sigma^+ \rightarrow X\ ^1\Sigma^+$ emission band systems of both isotopologues. The set of spectroscopic line measurements employed herein has been enlarged significantly from that of the previous work[2] by the inclusion of newer highly precise spectroscopic measurements. Furthermore, the use of purely analytical models for all radial functions represents a significant improvement that will certainly aid in the straightforward utilization of the results.

II. Method

We employ the Hamiltonian operator for a heteronuclear diatomic AB in a $^1\Sigma$ electronic state proposed by Coxon[14] on the basis of theoretical work by Watson.[29] For an isotopologue i, this is given as

$$H_i^{AB} = (2\mu_i^{at})^{-1}P_R^2 + U_i^{eff}(R) + B_i(R)[1 + q_i(R)]J(J+1) \tag{1}$$

where μ_i^{at} is the reduced mass defined in terms of atomic masses, P_R^2 is the nuclear kinetic energy operator, $U_i^{eff}(R)$ is the effective internuclear potential energy, $q_i(R)$ represents BO-breakdown effects, and $B_i(R) = \hbar^2/(2\mu_i^{at}R^2)$ is the radial part of the rotational energy operator. For HF isotopologues, $U_i^{eff}(R)$ can be written explicitly as

$$U_i^{eff}(R) = U^{BO}(R) + \frac{m_e U^H(R)}{M_i^H} + \frac{m_e U^F(R)}{M_i^F} \tag{2}$$

where $U^{BO}(R)$ is the BO-potential, $U^H(R)$ and $U^F(R)$ are BO-breakdown functions that contain $^1\Sigma \sim\ ^1\Sigma$ (homogeneous) interactions and adiabatic corrections, and m_e is the electron rest mass.

The J-dependent interactions arise from a combination of homogeneous and heterogeneous nonadiabatic interactions. As shown by Watson,[29] those separate contributions cannot be determined uniquely from consideration of zero-field transition energy data alone. The $q_i(R)$ function in eq 1, which collectively takes account of these interactions, can be partitioned into two atom-centered functions

Electronic States of Hydrogen Fluoride

J. Phys. Chem. A, Vol. 110, No. 19, 2006 **6263**

$$q_i(R) = \frac{m_e q^H(R)}{M_i^H} + \frac{m_e q^F(R)}{M_i^F} \tag{3}$$

Because there can be no isotopic substitution on the fluorine atomic center, it is not possible to achieve unique determinations of the three functions $U^{BO}(R)$, $U^H(R)$, and $U^F(R)$ in eq 2 from consideration of HF and DF spectroscopic data. In this case, we have employed the Le Roy "dominant isotopologue" approach,[30] in which the HF internuclear potential energy functions, $U_{HF(B)}^{eff}(R)$ and $U_{HF(X)}^{eff}(R)$, are obtained directly as the skeleton functions; it is then straightforward to obtain the $U^H(R)$ functions for both electronic states by considering simultaneously the input of DF data. The effective potentials for DF are then obtained as

$$U_{DF}^{eff}(R) = U_{HF}^{eff}(R) + m_e \frac{M^H - M^D}{M^H M^D} U^H(R) \tag{4}$$

where $U_{HF}^{eff}(R)$ includes a small inseparable contribution from the fluorine center.

It is important to emphasize that because $q_{HF}(R)$ and $q_{DF}(R)$ can be obtained uniquely in a fit of HF or DF data alone, respectively, and because $q_H(R)$ can be obtained from a combined HF/DF fit, the unique determination of $q_F(R)$ is possible here, despite the fact that there is no isotopic substitution at the fluorine atomic center.

In recent work on CO,[18] we were able to employ the Herman and Ogilvie[31] Hamiltonian operator, in which the kinetic energy operator is preceded by an atomic-mass-dependent Born–Oppenheimer breakdown term related to the slippage of electrons due to the vibrational motion. This radial function, along with an analogous function for rotational electron slippage effects, was determined for CO[18] by applying constraints related to the gyromagnetic ratio and the electric dipole moment. The advantage of using this framework is that there is allowance for separation of the adiabatic and homogeneous nonadiabatic corrections, which is not possible in the application of the Coxon/Watson Hamiltonian operator, eq 1. In the case of HF, however, use of this theoretical framework is precluded owing to the lack of isotopic substitution at the fluorine center. This, of course, is of no consequence to the quality of the fit; it simply means that the function $U^H(R)$ in eq 4 remains an admixture of adiabatic and homogeneous nonadiabatic effects. In the Herman–Ogilvie Hamiltonian operator this function would represent the pure adiabatic correction.

The mathematical models employed in the present work are very similar to those employed recently for carbon monoxide.[18] The HF isotopologue potential energy functions for both electronic states are modeled as MLJ oscillators[17]

$$U_{HF}^{eff}(R) = D_e \left[1 - \left(\frac{R_e}{R}\right)^n e^{-\phi(R)z}\right]^2 \tag{5}$$

where n is the power of the leading term in the long-range potential energy expression, $U(R) = D_e - C_n/R^n$, where $n = 6$ for the ground electronic state and $n = 1$ for the ion-pair long-range dependence of the $B\ {}^1\Sigma^+$ state, and z is the Ogilvie–Tipping[32] reduced internuclear coordinate, $z = 2(R - R_e)/(R + R_e)$. One of the distinct advantages of the MLJ model is that it offers a prescription for transforming the potential from the form of eq 5, to the long-range form, by defining the asymptotic value of the exponential function $\phi(R)$ as

$$\phi(\infty) = \frac{1}{2} \ln\left(\frac{2D_e R_e^n}{C_n}\right) \tag{6}$$

To prevent nonphysical behavior in $\phi(R)$ (and hence also in $U(R)$), the data-dependent portion of the function is joined smoothly to the asymptotic value $\phi(\infty)$ by means of a switching function, such that

$$\phi_z(R) = f_{sw}(R) \sum_{m=0} \phi_m z^m + [1 - f_{sw}(R)]\phi_z(\infty) \tag{7}$$

with

$$f_{sw}(R) = (1 + e^{\delta(R - R_{1/2})})^{-1} \tag{8}$$

where δ controls the damping strength and $R_{1/2}$ is the R value at which the switching function has a value of exactly 0.50. These parameters are constrained to sensible values that do not in any way impair the quality of the fit, while keeping the radial variation of $\phi(R)$ reasonable and free of pathological behavior. Selection of these values is facilitated to some degree by previous experience and often involves trial and error, albeit not extensive; the fitted parameter estimates ϕ_m adjust to accommodate a range of δ and $R_{1/2}$ values without affecting the goodness of the fit.

When $\phi(R)$ is represented in eq 7 with a high order polynomial in z, anomalous behavior is often found in the fitted function when extrapolating to R values lower than the radial range sampled by the data. As discussed in ref 21, a convenient resolution of this problem is afforded by a short linear extrapolation of $\phi(R)$ at $R < R_{inner}$. In the present work, this approach was required for the X state, for which $R_{inner} = 0.58$ Å.

The function $U^H(R)$ is represented by the model

$$U^H(R) = f_{sw}^{U^H}(R) \sum_{m=1} u_m^H z^m + u_\infty^H \left[1 - \frac{f_{sw}^{U^H}(R)}{f_{sw}^{U^H}(R_e)}\right] \tag{9}$$

subject to the arbitrary condition $U^H(R_e) = 0$. Finally, the functions $q^H(R)$ and $q^F(R)$ are modeled as

$$q^H(R) = f_{sw}^{q^H}(R) \sum_{m=1} q_m^H x^m \tag{10}$$

$$q^F(R) = f_{sw}^{q^F}(R) \sum_{m=1} q_m^F x^m \tag{11}$$

where x is the reduced variable $(R - R_e)/R_e$; the switching functions in eqs 10 and 11 ensure that $q^H(R)$ and $q^F(R)$ decay to zero as R tends to infinity, in accord with the theoretical expectation.[33]

One remaining quantity that must be considered is the electronic term value of the $B\ {}^1\Sigma^+$ state, along with its isotopic dependence. We can write for the two electronic states the following electronic term value expressions

$$T_i^{el}(X) = T_{BO}^{el}(X) + \frac{d_X^H}{M_i^H} + \frac{d_X^F}{M_i^F} \tag{12}$$

and

$$T_i^{el}(B) = T_{BO}^{el}(B) + \frac{d_B^H}{M_i^H} + \frac{d_B^F}{M_i^F} \tag{13}$$

TABLE 1: Experimental Line Position Data^a for the B $^1\Sigma^+$ and X $^1\Sigma^+$ States of HF and DF

isotopologue	type	accuracy/cm^{-1}	Δv	v_{max}	J_{max}	no. lines	authors	year
HF (X)	far IR/heterodyne	$(0.15-200) \times 10^{-5}$	0	0	33	17	Jennings et al.	1987, 1988
HF (X)	*tunable far-IR	$(0.58-1.6) \times 10^{-5}$	0	0	7	2	Odashima et al.	1999
HF (X)	*FTIR emission	0.0002	0	0	25	13	Hedderich et al.	1991
HF (X)	*FTIR at 2300 °C	0.0005	0	4	35	59	Ram et al.	1996
HF (X)	*IR absorption	0.001−0.01	0	2	39	9	Lemoine and Demuynck	1987
HF (X)	laser emission	0.003	0	3	24	20	Sengupta et al.	1979
HF (X)	*laser emission	0.025	0	3	30	27	Deutsch	1967b
HF (X)	far-IR absorption	0.05−0.08	0	0	17	17	Mason and Neilsen	1967
HF (X)	laser emission	0.10	0	2	33	19	Cuellar and Pimentel	1979
HF (X)	far-IR laser emission	0.20	0	3	25	12	Akitt and Yardley	1970
HF (X)	far-IR absorption	0.20	0	0	11	11	Rothschild	1964
HF (X)	laser emission	0.40	0	5	41	75	Revich and Stankevich	1966
HF (X)	*heterodyne	3.3×10^{-5}	1	1	6	5	Goddon et al.	1991
HF (X)	*FTIR emission	0.0002	1	2	16	45	Le Blanc et al.	1994
HF (X)	absorption	0.0005	1	1	12	22	Guelachvili	1976
HF (X)	*FTIR at 2300 °C	0.0005	1	5	28	116	Ram et al.	1996
HF (X)	IR laser	0.005	1	6	15	49	Sengupta et al.	1979
HF (X)	IR absorption	0.01	1	1	15	29	Webb and Rao	1968
HF (X)	IR absorption	0.03	1	1	10	19	Herget et al.	1962
HF (X)	flame emission	0.075−0.12	1	3	28	97	Mann et al.	1961
HF (X)	laser emission	0.10−0.12	1	3	15	31	Deutsch	1967a
HF (X)	FTIR absorption	0.001	2	2	9	18	Guelachvili	1976
HF (X)	IR absorption	0.016	2	2	9	15	Webb and Rao	1968
HF (X)	IR absoption	0.04	2	2	9	16	Herget et al.	1962
HF (X)	flame emission	0.12−0.15	2	6	28	214	Mann et al.	1961
HF (X)	*laser absorption	0.003	3	3	10	17	Sasada	1994
HF (X)	absorption	0.01	3	3	9	16	Fishburne and Rao	1966
HF (X)	flame emission	0.10−0.15	3	6	22	110	Mann et al.	1961
HF (X)	*absorption	0.01	4	4	7	13	Fishburne and Rao	1966
HF (X)	flame emission	0.12	4	8	24	185	Mann et al.	1961
HF (X)	*absorption	0.02	5	5	5	9	Fishburne and Rao	1966
HF (X)	flame emission	0.15	5	9	22	131	Mann et al.	1961
HF ($B - X$)	UV emission	0.03				1797	Di Lonardo and Douglas	1973
DF (X)	submm. absorption	0.00002	0	0	1	1	De Lucia et al.	1971
DF (X)	*FT far-IR absorption	0.0001	0	0	9	8	Hajigeorgiou	1991
DF (X)	*FTIR at 2300 °C	0.0005	0	3	48	89	Ram et al.	1996
DF (X)	*FTIR	0.00005	1	1	12	25	Ram et al.	1996
DF (X)	*FTIR at 2300 °C	0.0005	1	5	32	151	Ram et al.	1996
DF (X)	IR laser emission	0.004	1	4	17	58	Sengupta et al.	1979
DF (X)	*absorption	0.01	1	1	13	16	Spanbauer et al.	1965
DF (X)	*laser emission	0.08	1	4	17	30	Deutsch	1967a
DF (X)	absorption	0.01	2	2	11	19	Spanbauer et al.	1965
DF ($B - X$)	UV emission	0.04				1544	Coxon and Hajigeorgiou	1989
DF ($B - X$)	UV emission	0.04				981	Coxon and Hajigeorgiou	1990
	total no. Lines					6157		

^{a} For each data set, the table shows the number of line positions employed in the least-squares fits of the present work; Δv is the change in vibrational number for transitions within the X state; the maximum vibrational and rotational quantum numbers for the set are given as v_{max} and J_{max}. Data sets not available or not considered in the previous work[2] are flagged with an asterisk.

so that the separation between electronic states B and X for isotopologue i is

$$T_i^{el}(B) - T_i^{el}(X) = \Delta T_{BO}^{el} + \frac{\Delta d^H}{M_i^H} + \frac{\Delta d^F}{M_i^F} \qquad (14)$$

which can also be written as

$$T_i^{el}(B) - T_i^{el}(X) = \Delta T_{eff}^{el} + \frac{\Delta d^H}{M_i^H} \qquad (15)$$

to indicate that the parameter Δd^F is indeterminable. The two determinable parameters in eq 15 are ΔT_{eff}^{el} and Δd^H.

The global treatment of HF and DF data is carried out by means of a weighted nonlinear least-squares fit to the Hamiltonian parameters. The partial derivatives required in the method are calculated accurately by numerical integration according to the Hellmann−Feynman theorem (see eq 25 of ref 18). Radial functions for the X state were obtained at 12001 grid points in the range 0.4−6.4 Å, corresponding to a mesh size of 0.0005

Å; for the B state, 4001 points were employed over the range 1.0−5.0 Å with a mesh size of 0.001 Å. Tests were performed to ensure that the radial ranges and mesh sizes were defined such that error in the derived eigenvalues was negligible with respect to the uncertainties in the measured line positions. Fundamental constants and atomic masses were taken from the most recent compilations.[34,35]

III. Spectroscopic Data

In our previous global analysis of HF and DF data,[2] we employed a total of 5213 spectroscopic line positions. The current data set is increased by 944 to a total of 6157 line positions. Many of the newly employed line positions have been measured with significantly higher precision compared to previously existing data having the same vibrational/rotational excitation, and/or enlarge markedly the range of rotational excitation. The greatest portion of the line position data is derived from the analyses of the B $^1\Sigma^+ \rightarrow X$ $^1\Sigma^+$ emission band systems of HF and DF.[2,36,37] These analyses contribute 4322 line positions, or close to 70% of the total.

Electronic States of Hydrogen Fluoride

J. Phys. Chem. A, Vol. 110, No. 19, 2006 **6265**

TABLE 2: Fitted Potential Function Parameters[a] for the $X\ ^1\Sigma^+$ and $B\ ^1\Sigma^+$ States of HF

parameter	$X\ ^1\Sigma^+$	$B\ ^1\Sigma^+$
$\delta/\text{Å}^{-1}$	[3.70]	[3.50]
$R_{1/2}/\text{Å}$	[3.00]	[3.80]
ϕ_0	$-3.9672377_{2059}(4)$	$0.33378_{0178}(1)$
ϕ_1	$0.796334_{1064}(8)$	$0.7497_{1091}(1)$
ϕ_2	$0.16100_{9057}(4)$	$-0.9546_{4843}(6)$
ϕ_3	$0.5552_{8385}(3)$	$-1.099_{2640}(4)$
ϕ_4	$0.384_{6146}(1)$	$2.28_{4551}(1)$
ϕ_5	$0.630_{9591}(7)$	$4.55_{2909}(6)$
ϕ_6	$0.05_{0499}(2)$	$-5.3_{6981}(1)$
ϕ_7	$-3.68_{9526}(7)$	$-12.1_{8157}(4)$
ϕ_8	$9.1_{8380}(2)$	$13.1_{3814}(3)$
ϕ_9	$16.0_{5901}(3)$	$22._{3372}(1)$
ϕ_{10}	$-79.7_{9459}(9)$	
ϕ_{11}	$53._{5575}(1)$	
ϕ_{12}	$165.6_{3607}(5)$	
ϕ_{13}	$-354._{0128}(2)$	
ϕ_{14}	$262._{6046}(1)$	
ϕ_{15}	$-70.1_{1957}(4)$	
D_e/cm^{-1}	[49361.6]	[46872.0]
$R_e/\text{Å}$	$0.91683896_{4172}(2)$	$2.090943_{5382}(4)$
$R_{inner}/\text{Å}$	0.58	
$\Delta T_{eff}^{el}/\text{cm}^{-1}$		$84783.643_{86}(9)$
$\Delta d^{H}/\text{u cm}^{-1}$		$-6.77_{1228}(3)$

[a] The values of R_e and the sets of ϕ_i parameters refer to the effective potentials of the X and B states of HF, see text. Entries in square brackets denote constrained parameters; entries in parentheses correspond to estimated one standard errors, in units of the last nonsubscripted digit of the corresponding parameter.

Table 1 contains a concise summary of the current data set. For HF, there are pure rotational line position measurements from many sources,[38–50] and vibration–rotational line position measurements[51–59] obtained by employing a variety of techniques, including FTIR emission/absorption, infrared laser-induced fluorescence, classical spectrographic flame emission, and heterodyne methods. Finally, for HF, the set of line positions measured by Di Lonardo and Douglas[36] for the $B\ ^1\Sigma^+ \rightarrow X\ ^1\Sigma^+$ emission band system completes the data set. For DF, pure rotational line positions are available from the work of De Lucia et al.,[60] Hajigeorgiou's Ph.D. thesis,[61] and Ram et al.[42] Vibration–rotational data were obtained from the analyses of Ram et al.,[42] Sengupta et al.,[44] Spanbauer et al.,[62] and Deutsch.[57] Investigation and analysis of the extensive ultraviolet $B\ ^1\Sigma^+ \rightarrow X\ ^1\Sigma^+$ emission band system of DF was undertaken by Coxon and Hajigeorgiou.[2,37]

The extent of the vibrational index for the spectroscopic data included in the present global fits is $v'' = 0$–19 for HF(X), $v'' = 0$–26 (excluding levels with $v'' = 6$–8) for DF(X), $v' = 0$–10 for HF(B), and $v' = 0$–7 for DF(B).

IV. Results and Discussion

The comprehensive least-squares fit of 6157 HF/DF spectroscopic line positions gave a reduced standard deviation of $\hat{\sigma} = 1.028$. This statistical indicator gives the weighted average of the residuals (observed − calculated) relative to their experimental uncertainties, so that a result of $\hat{\sigma} \approx 1.0$ is ideal for a data set that is free of systematic error, and for which the associated uncertainties have been estimated realistically. The total number of adjustable parameters in the fit was 54, of which 36 characterize the $X\ ^1\Sigma^+$ ground electronic state and the remaining 18 describe the excited $B\ ^1\Sigma^+$ ion-pair state. The estimated potential function parameters and their standard errors for the X and B states are listed in Table 2. For both states, the dissociation energies were constrained to estimated values that are more precise and reliable than those found from our least-

TABLE 3: Born−Oppenheimer Breakdown Functions[a] for the $X\ ^1\Sigma^+$ and $B\ ^1\Sigma^+$ States of HF

parameter	$X\ ^1\Sigma^+$	$B\ ^1\Sigma^+$
$\delta/\text{Å}^{-1}$	[8.00]	[4.00]
$R_{1/2}/\text{Å}$	[2.50]	[2.70]
$m_e u_\infty^{H}/\text{u cm}^{-1}$	$27.42_{682}(9)$	$-21.6_{172}(5)$
$10^5 u_1^{H}/\text{cm}^{-1}$	$1.1840_{711}(5)$	$-1.30_{3683}(2)$
$10^5 u_2^{H}/\text{cm}^{-1}$	$-2.870_{925}(2)$	$1.07_{3226}(2)$
$10^5 u_3^{H}/\text{cm}^{-1}$	$3.68_{864}(4)$	$4.1_{5468}(3)$
$10^5 u_4^{H}/\text{cm}^{-1}$	$-1.2_{0288}(2)$	$3.1_{5968}(9)$
$10^5 u_5^{H}/\text{cm}^{-1}$	$-0.5_{0663}(4)$	
$10^5 u_6^{H}/\text{cm}^{-1}$	$-12._{8253}(1)$	
$10^5 u_7^{H}/\text{cm}^{-1}$	$55._{5406}(3)$	
$10^5 u_8^{H}/\text{cm}^{-1}$	$-73._{7058}(3)$	
$10^5 u_9^{H}/\text{cm}^{-1}$	$31._{2377}(1)$	
$\delta/\text{Å}^{-1}$	[3.00]	
$R_{1/2}/\text{Å}$	[4.50]	
q_1^{H}	$-0.111_{718}(3)$	
q_2^{H}	$-0.71_{8557}(5)$	
q_3^{H}	$0.0_{64555}(1)$	
q_4^{H}	$-0.2_{4251}(1)$	
q_5^{H}	$-0.08_{0841}(7)$	
q_6^{H}	$-0.14_{5375}(1)$	
$\delta/\text{Å}^{-1}$	[3.00]	
$R_{1/2}/\text{Å}$	[4.50]	
q_1^{F}	$-4.0_{1777}(5)$	
q_2^{F}	$9._{33428}(1)$	
q_3^{F}	$-5.4_{6394}(5)$	

[a] Entries in square brackets denote constrained parameters; entries in parentheses correspond to estimated one standard errors, in units of the last nonsubscripted digit of the corresponding parameter.

squares fit. It is essential to emphasize that these listed parameters describe directly the potentials of the HF isotopologue. Using eq 4 and the $U^{H}(R)$ functions, the corresponding potentials for DF can be readily constructed. The BO-breakdown functions $U^{H}(R)$ for both electronic states, and $q^{H}(R)$ and $q^{F}(R)$ for the X state, can be constructed from the parameters listed in Table 3. Statistically significant determinations of the $q^{H}(R)$ and $q^{F}(R)$ functions for the B state could not be obtained, indicating the lack of significant J-dependent perturbations in this state over the range of vibrational excitation sampled in the spectrographic ultraviolet flame emission data.

Figure 2 shows the $\phi(R)$ functions for both electronic states. Both functions are seen to vary smoothly over the radial range covered by the data, shown in solid lines, and to extrapolate sensibly in both directions, as shown by the dashed lines. At large R, the functions reach asymptotes that can be calculated easily from eq 6 and the known values of C_n. For the ground electronic state, $C_6 = 37425$ cm^{-1} Å^6 from the analysis of Zemke et al.[63] Assuming a simple ion-pair Coulombic interaction at long-range for the $B\ ^1\Sigma^+$ electronic state, we obtain $C_1 = 116\,110$ cm^{-1} Å, leading to the *approximate* estimates for the asymptotes, $\phi_X(\infty) \approx 0.2245$ and $\phi_B(\infty) \approx 0.2618$.

The $U^{H}(R)$ function for the X state is shown in Figure 3, along with selected points from the analogous function obtained in our 1990 analysis.[2] The agreement between the two functions is very good over most of the radial range, but it is clear that while the 1990 function exhibits pathological behavior at large R, the function obtained in the present work approaches an asymptote smoothly and sensibly. In our previous work[2] there
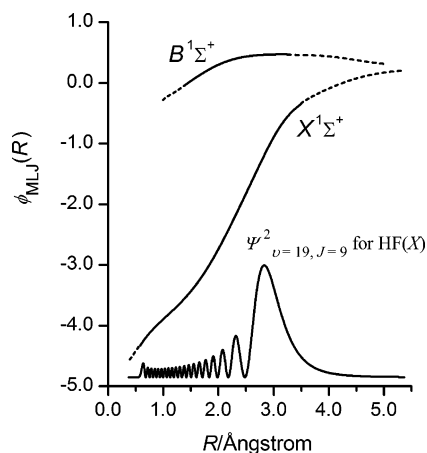
Figure 2. The exponential $\phi_{MLJ}(R)$ functions of eq 5 (see text) for the $X\ ^1\Sigma^+$ and $B\ ^1\Sigma^+$ states of HF, as defined by the parameters in Table 2. The solid regions of the curves correspond to radial ranges defined by the available data, and extrapolations are indicated by broken curves. Also shown in the lower part of the diagram is the square of the radial wave function of the $X, v = 19$ vibrational level for $J = 9$, the highest observed level for HF(X).
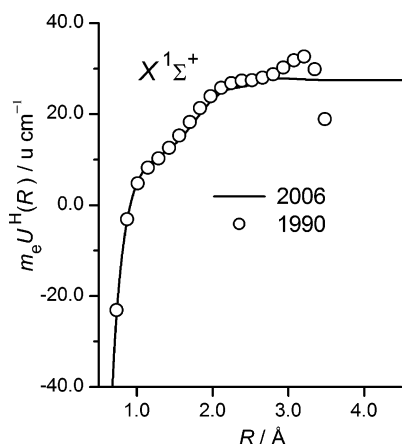

Figure 3. The solid line shows the $U^H(R)$ isotopically invariant function of eq 4 (see text) for the $X\ ^1\Sigma^+$ electronic state of HF obtained in the present work. The open circles represent selected points from the function obtained in previous work.[2] The two functions agree well for $R \leq 2.7$ Å, but for $R > 2.7$ Å, pathological behavior of the 1990 function owing to lack of provision for sensible extrapolation leads to large systematic differences.

was no particular consideration for the behavior of $U^H(R)$ at large R, and the observed pathological behavior of the function simply indicates that the model employed previously was unsatisfactory at modeling the physical realities of the problem. In the present work, an asymptote is reached with the aid of a switching function, and this is related directly to the difference between the dissociation energies of HF and DF. From experiments using threshold ion-pair production spectroscopy (TIPPS),[64] the dissociation energies of both isotopologues are known precisely as $D_e(HF) = 49361.6 \pm 0.9$ cm^{-1} and $D_e(DF) = 49349.2 \pm 0.9$ cm^{-1}, giving a difference $\Delta D_e = 12.4 \pm 0.5$ cm^{-1}, which is the value quoted in ref 64. The asymptote of our $U^H(R)$ function is given by the parameter in Table 3, $m_e u_\infty^H(X) = 27.4 \pm 0.1$ cm^{-1}. This asymptote must be multiplied by the factor $(M_H^{-1} - M_D^{-1})$ in order to be directly comparable to the experimental result. Performing this calculation gives the estimate $\Delta D_e = 13.7 \pm 0.1$ cm^{-1}, which lies outside the combined standard errors of the two values. In any case, our error estimate of ± 0.1 cm^{-1} cannot be regarded as statistically rigorous because it takes no account of model error
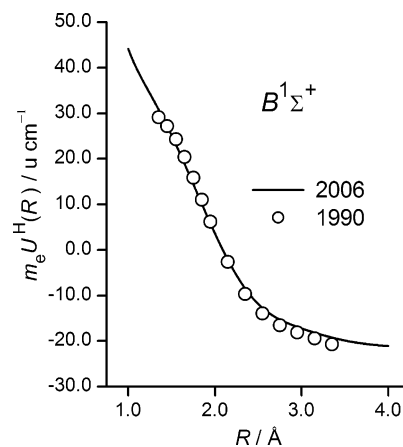

Figure 4. The solid line shows the $U^H(R)$ isotopically invariant function of eq 4 (see text) for the $B\ ^1\Sigma^+$ electronic state of HF obtained in the present work. The open circles represent selected points from the function obtained in previous work.[2] As for the X state, excellent agreement between the two functions is obtained for small displacements from the equilibrium internuclear separation, but the agreement deteriorates at large R values owing to the lack of provision for a sensible extrapolation in the 1990 function.

that might arise for slightly different values of δ and $R_{1/2}$ in the relevant switching function. It is also important to note that attempts to constrain the ΔD_e value to the TIPPS estimate gave a significantly poorer least-squares fit, particularly for ground-state vibrational levels close to the dissociation limit. Another possible source of error in our fitted ΔD_e estimate is the fact that for DF(X) vibrational levels with $v'' = 6-8$ are not sampled by the experimental data and their energies are essentially interpolated. It would be of much interest in the future to carry out model calculations in order to assess the effects on the ΔD_e estimate of varying the constrained values for δ and $R_{1/2}$ in the switching function, and having interpolated vibrational levels.

Figure 4 shows the analogous function $U^H(R)$ for the excited state. As before, the solid line represents the function obtained in the present work and the open circles represent selected points from the 1990 function. The agreement is quite reasonable over the full radial range covered in the 1990 work. The current function, however, has the advantage of being constrained to approach an asymptote, as expected theoretically. The asymptote obtained in the present work is negative, which implies that for the excited $B\ ^1\Sigma^+$ state, the dissociation energy of DF is greater than that of HF. This may be related to the fact that the $B\ ^1\Sigma^+$ state dissociates to ionic products, and is similar to the situation encountered for the $B\ ^1\Sigma^+$ state of HCl.[4]

Figure 5 shows the interesting comparison between the HF potentials of the present work with the functions obtained in the 1990 work. The solid curve represents the difference $U_{2006}^X(R) - U_{1990}^X(R)$ for the $X\ ^1\Sigma^+$ state, and the broken curve represents the analogous difference for the B state. For the ground state, the difference remains small over the radial range $R = 0.75-2.5$ Å. However, for $R > 2.50$ Å, the difference increases significantly and displays oscillatory structure. This trend almost certainly arises from the application of localized Gaussian correction functions in the previous work[2] for the determination of the total IPA corrections to the trial potential. Oscillatory structure caused by the use of localized Gaussian correction functions in previous work[2] is also observed for the $B\ ^1\Sigma^+$ state, as can be seen in Figure 5. We believe that these comparisons reveal with a high degree of confidence the significant improvements achieved in the present work in representing radial functions, particularly with increasing internuclear distance.
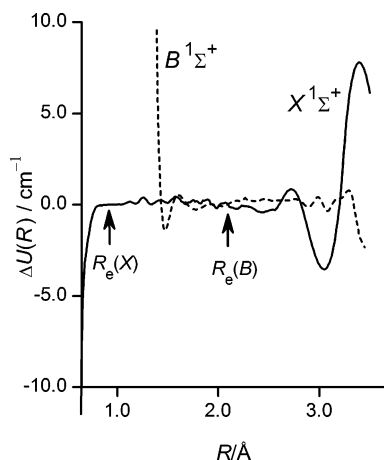
Electronic States of Hydrogen Fluoride

J. Phys. Chem. A, Vol. 110, No. 19, 2006 **6267**

Figure 5. The solid line indicates the difference function $\Delta U(R) = U_{2006}^{X}(R) - U_{1990}^{X}(R)$ for the HF $X\ ^1\Sigma^+$ potential, where $U_i^X(R)$ are the potentials determined in the present work and in the earlier work;[2] the broken line represents the analogous difference function for the $B\ ^1\Sigma^+$ state. For the X state, the $\Delta U(R)$ function is small in magnitude over most of the range of R, but becomes oscillatory at large R, owing to the use of localized Gaussian correction functions (see text) in the previous work.[2] Smaller oscillations are also evident at large R in the $\Delta U(R)$ function for the B state.
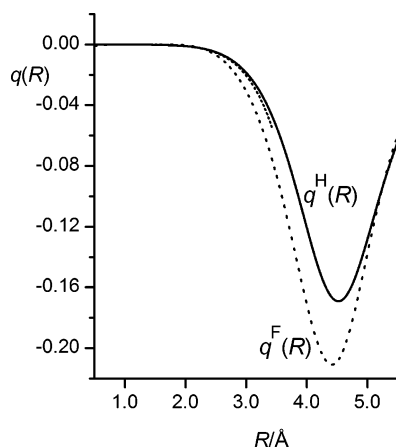

Figure 6. The solid curve represents the $X\ ^1\Sigma^+$ state $q^H(R)$ function of eq 10 (see text), and the dashed curve represents the $q^F(R)$ function of eq 11 (see text). The two functions are forced to approach an asymptote of zero at large R, in accord with theoretical expectations (see text). For comparison purposes, the $q^{HF}(R)$ function obtained in the previous work[2] is shown by the dotted curve lying close to the $q^H(R)$ function.

Figure 6 displays the radial variation of the ground state $q^H(R)$ and $q^F(R)$ functions. These have shapes similar to those obtained previously[2] for the $q(R)$ function, where they are very small in magnitude for $R < 2$ Å, but become increasingly negative at higher R. The current functions are switched to a value of zero in the region where the data no longer have any effect, as can be seen in Figure 6. The theoretical interpretation and radial behavior of $q(R)$ have been discussed previously.[2] One component of $q(R)$ arises from heterogeneous ($^1\Sigma \sim {}^1\Pi$) electronic state coupling. The increasing proximity of the $A\ ^1\Pi$ repulsive electronic state to the ground $X\ ^1\Sigma^+$ electronic state, as the latter approaches its dissociation limit (see Figure 1), creates increasingly negative contributions to the rotational energies of the ground state so that the ground state rotational levels are effectively "pushed down", in accord with the expectation from conventional second-order perturbation theory. This interaction explains clearly the increasingly negative values taken on by $q(R)$ as R increases.

The concept of molecular constants has served well the spectroscopic community over many decades. This formulation received theoretical support early on, particularly through the pioneering work of Dunham,[65] which placed the existence of such entities on a firm theoretical footing. Unfortunately, in practice, in analyses of the spectra of light diatomic molecules, and especially hydrides, the estimated molecular parameters frequently lack a strict mechanical meaning. This shortcoming renders the molecular parameters unsuitable for extrapolating to higher J with any degree of reliability. In past work[4,18] we have demonstrated that reliable molecular constants may be calculated a posteriori using the radial functions obtained in such work in association with Rayleigh–Schrödinger perturbation theory. Such calculated constants are then the true perturbation series coefficients of an expansion in the variable $J(J+1)$, as defined by quantum mechanics. Furthermore, they do not suffer from the effects of interparameter statistical correlations, nor do they contain contributions from omitted higher-order parameters, unlike those obtained in practical applications where truncation of the $J(J+1)$ power series is unavoidable. Accordingly, we have calculated molecular constants for the $X\ ^1\Sigma^+$ and the $B\ ^1\Sigma^+$ electronic states of HF and DF. Because of the large volume of tables containing such entries, we have decided to present herein only the molecular constants for the $X\ ^1\Sigma^+$ states that relate to the vibrational levels sampled by the available vibration–rotational data. We present the relevant constants for HF and DF in Tables 4 and 5, respectively. Molecular constants for all observed vibrational levels for both isotopologues and both electronic states are available as Supporting Information. In order for some of the new HF rotationally hot infrared data[42] to be reproduced to within the experimental uncertainties, we have found it necessary to not only include a calculation of the octic and nonic order constants P_v and Q_v that were not considered previously but also extend the expansion to include the 10th- and 11th-order terms R_v and S_v for the X states of HF and DF, to obtain eigenvalues that reproduce the highly precise spectroscopic line positions within the experimental uncertainties. The observation that in the experimental analysis,[42] such spectra were represented adequately by up to a 6th-order expansion in $J(J+1)$, indicates clearly the presence of the aforementioned effects that render the experimentally derived constants as effective values only.

The calculation of the 10th- and 11th-order centrifugal distortion constants (CDC) R_v and S_v requires the estimation of the 5th-order correction to the wave function, and is thus very much sensitive to numerical noise. However, because of the high degree of smoothness in our radial functions, problems of this sort were neither expected nor encountered in the actual calculations. In addition to their other advantages, our molecular constants are expected to be the most reliable in extrapolating to higher J. Their only apparent drawback is that they do not include any estimate of statistical uncertainty; it is not obvious how proper account of error propagation from the estimated parameters of our least-squares fit could be accommodated in this calculation. The estimation of the number of significant digits for the centrifugal distortion constants has been achieved in two ways. First, with known data precision and the extent of rotational excitation, it is possible to obtain a relative truncation of the constants. However, this does not take into account any possible shortcomings associated with the particular method of calculation of the constants. In other words, the absolute accuracy of the CDC calculation methodology must be assessed. The assessment of absolute accuracy in the calculation of centrifugal distortion constants was the subject of a recent

TABLE 4: Molecular Constants (cm^{-1}) for the $X\ ^1\Sigma^+$ State of HF

v	G_v	B_v	10^3D_v	10^7H_v	$10^{11}L_v$	$10^{15}M_v$	$10^{19}N_v$	$10^{22}O_v$	$10^{25}P_v$	$10^{29}Q_v$	$10^{32}R_v$	$10^{35}S_v$
0	2050.761082	20.559730458	2.119962810	1.63803772	−1.5587674	1.592244	−2.05007	0.235884	−0.032821	0.03555	0.00551	0.0002
1	6012.183537	19.787476946	2.06379542	1.5910548	−1.555203	1.544336	−2.07143	0.21219	−0.03287	0.0490	0.00799	−0.0227
2	9801.55456	19.034963756	2.01019848	1.5403308	−1.556565	1.47013	−2.0945	0.22395	−0.04261	−0.1730	0.2087	−0.1168
3	13423.56507	18.300604183	1.95957337	1.4847830	−1.564264	1.38819	−2.2783	0.1538	0.0674	−1.118	0.649	−0.245
4	16882.40268	17.582569664	1.91238665	1.423507	−1.58553	1.2760	−2.327	−0.238	0.378	−2.87	1.19	−0.30
5	20181.70002	16.878770194	1.8692437	1.354870	−1.6256	1.0771	−1.870	−1.164	0.902	−5.05	1.50	−0.11
6	23324.465	16.1867712	1.830926	1.27626	−1.6882	0.7080	−0.674	−2.730	1.558	−6.90	1.09	0.51
7	26312.990	15.5036893	1.798433	1.18378	−1.7806	0.0635	1.229	−4.908	2.166	−7.42	−0.53	1.66
8	29148.739	14.8260630	1.773078	1.07167	−1.9189	−0.9829	3.431	−7.596	2.458	−5.70	−3.76	3.28
9	31832.203	14.1496729	1.756639	0.93131	−2.1363	−2.6007	4.974	−10.753	2.064	−1.51	−8.82	4.90

TABLE 5: Molecular Constants (cm^{-1}) for the $X\ ^1\Sigma^+$ State of DF

v	G_v	B_v	10^4D_v	10^8H_v	$10^{12}L_v$	$10^{17}M_v$	$10^{21}N_v$	$10^{25}O_v$	$10^{29}P_v$	$10^{33}Q_v$	$10^{37}R_v$	$10^{41}S_v$
0	1490.33540	10.860344769	5.87468735	2.3852372	−1.188680	6.397970	−4.30750	2.6347	−1.805	0.645	−0.717	3.24
1	4396.99697	10.564028043	5.76098212	2.3367700	−1.186116	6.28143	−4.3003	2.117	−1.392	3.143	−8.921	9.34
2	7212.15320	10.273325569	5.65079218	2.2858331	−1.184902	6.04293	−4.1673	2.440	−4.326	7.805	−6.256	−22.28
3	9937.68872	9.987946445	5.54449231	2.231415	−1.18444	5.8079	−4.4454	3.594	−7.076	5.194	20.842	−105.55
4	12575.35897	9.707559908	5.4424906	2.173211	−1.18730	5.6242	−5.1493	4.713	−6.150	−12.199	81.416	−242.24
5	15126.78000	9.43180391	5.3452748	2.110928	−1.19651	5.4782	−6.0138	4.485	1.631	−49.541	177.813	−419.55

TABLE 6: Molecular Constants (cm^{-1}) for $v = 0$ of HF($X\ ^1\Sigma^+$)

constant	estimate	reference
B_0	20.559730458	present work
	20.55973066(42)	42
	20.55973002(33)	39
D_0	$2.11996281 \times 10^{-3}$	present work
	$2.119960(15) \times 10^{-3}$	42
	$2.119880(13) \times 10^{-3}$	39
H_0	1.6380377×10^{-7}	present work
	$1.63793(64) \times 10^{-7}$	42
	$1.63380(67) \times 10^{-7}$	39
L_0	$-1.558767 \times 10^{-11}$	present work
	$-1.5528(111) \times 10^{-11}$	42
	$-1.4810(67) \times 10^{-11}$	39
M_0	1.59224×10^{-15}	present work
	$1.480(85) \times 10^{-15}$	42
	$0.981(27) \times 10^{-15}$	39
N_0	-2.0501×10^{-19}	present work
	$-1.23(24) \times 10^{-19}$	42
O_0	2.359×10^{-23}	present work

TABLE 7: Potential Listings^a for the $X\ ^1\Sigma^+$ States of HF and DF

	HF			DF		
v	G_v	$R_{\min}$	$R_{\max}$	G_v	$R_{\min}$	$R_{\max}$
0	2050.761	0.834163	1.020549	1490.335	0.845388	1.003647
1	6012.184	0.784494	1.113084	4396.997	0.801118	1.078757
2	9801.555	0.754787	1.186890	7212.153	0.774063	1.137282
3	13423.565	0.733063	1.254038	9937.689	0.753945	1.189532
4	16882.403	0.715901	1.318065	12575.359	0.737811	1.238498
5	20181.700	0.701759	1.380651	15126.780	0.724327	1.285554
6	23324.465	0.689795	1.442817	17593.418	0.712759	1.331485
7	26312.990	0.679490	1.505305	19976.577	0.702653	1.376804
8	29148.739	0.670502	1.568746	22277.384	0.693706	1.421880
9	31832.203	0.662594	1.633758	24496.769	0.685706	1.467007
10	34362.711	0.655596	1.701018	26635.445	0.678498	1.512438
11	36738.178	0.649384	1.771347	28693.883	0.671963	1.558408
12	38954.760	0.643865	1.845807	30672.281	0.666013	1.605150
13	41006.411	0.638973	1.925873	32570.528	0.660575	1.652911
14	42884.271	0.634664	2.013696	34388.157	0.655594	1.701968
15	44575.871	0.630910	2.112618	36124.286	0.651025	1.752641
16	46064.051	0.627701	2.228205	37777.551	0.646831	1.805319
17	47325.477	0.625045	2.370673	39346.017	0.642984	1.860486
18	48328.360	0.622975	2.561907	40827.071	0.639461	1.918769
19	49026.360	0.621555	2.867731	42217.294	0.636245	1.980994
20	49340.055	0.620922	3.862298	43512.296	0.633325	2.048290
21				44706.517	0.630693	2.122255
22				45792.980	0.628347	2.205240
23				46762.975	0.626291	2.300892
24				47605.634	0.624532	2.415300
25				48307.241	0.623087	2.559823
26				48849.571	0.621982	2.760332
27				49204.293	0.621265	3.109782

^{a} Vibrational level energies are in cm^{-1} units; internuclear distances are in Å units.

investigation by Hajigeorgiou,[66] where exact analytical expressions were derived for the centrifugal distortion constants up to 11th-order, using the well-known closed-form expression for the rovibrational energy of a Kratzer-Fues oscillator. It appears that the calculated constants reproduce the vibration−rotational data very well; 1835 such spectroscopic lines are reproduced with $\hat{\sigma} = 1.014$, which is most satisfactory. A closer inspection of the residuals (observed − calculated) indicates that for the HF $v = 2$ pure rotational data of Lemoine and Demuynck (see Table 1), the $R(35)$ and $R(38)$ lines are reproduced with residuals that are 4.7 and 13.1 times the experimental uncertainty, whereas in the least-squares fit these residuals were 0.2 and −0.4, respectively. This is evidence of one of two things: either (a) the 10th- and 11th-order constants R_v and S_v are not calculated properly by Hutson's method[67] or (b) 6th-order wave function corrections need to be considered. Because the radial functions obtained in this work are very smooth and continuous throughout, we tend to favor the second explanation. However, we felt that the effort required in including 12th- and 13th-order centrifugal distortion constants would be disproportionate to the advantage gained in reproducing just two spectroscopic lines to within their experimental precision. It is also obvious that there is sufficient evidence for the convergence of the $J(J+1)$ perturbation expansion for the ground states of HF and DF.

A direct comparison between experimental and calculated molecular constants for $v = 0$ in HF ($X\ ^1\Sigma^+$) is shown in Table 6. The agreement is clearly excellent for the lower-order constants, but deteriorates, as expected, at higher-order.

In previous work,[2] we presented RKR-style listings of the potential energy functions for HF and DF. Although it is now considerably simpler to construct the analytical potential functions from the tabulated parameters, many applications require potentials that are not necessarily of the high degree of accuracy found in the fitted functions. In these cases, RKR-style listings of the potential functions would still be of much value, and indeed a close examination of the citation record of our previous publication[2] showed that such listings proved helpful to many investigators. As such, the potentials for the $X\ ^1\Sigma^+$ and $B\ ^1\Sigma^+$ states of HF and DF are presented in Tables 7 and 8. The

Electronic States of Hydrogen Fluoride

J. Phys. Chem. A, Vol. 110, No. 19, 2006 **6269**

TABLE 8: Potential Listings[a] for the $B\ ^1\Sigma^+$ States of HF and DF

	HF			DF		
v	G_v	R_{min}	R_{max}	G_v	R_{min}	R_{max}
0	572.139	1.924803	2.274854	416.295	1.948021	2.245715
1	1695.940	1.810674	2.425969	1238.049	1.849520	2.370677
2	2785.322	1.735157	2.540114	2041.458	1.784101	2.463432
3	3841.457	1.675280	2.640211	2826.974	1.732137	2.543588
4	4865.487	1.624448	2.732805	3595.042	1.687979	2.616774
5	5858.512	1.579670	2.820847	4346.096	1.649059	2.685538
6	6821.594	1.539294	2.905960	5080.563	1.613956	2.751284
7	7755.760	1.502301	2.989148	5798.856	1.581787	2.814880
8	8662.007	1.468017	3.071084			
9	9541.317	1.435976	3.152241			
10	10394.670	1.405853	3.232966			

[a] Vibrational level energies are in cm^{-1} units; internuclear distances are in Å units.

"turning points" of particular vibrational levels were calculated exactly to the desired degree of accuracy from the analytical functions.

The highest observed vibrational level for the ground X state of HF is $v = 19$. This level lies approximately $336\ cm^{-1}$ below the dissociation limit, or at an energy of 99.3% of D_e. Given the expected reliability at long-range of our potential energy function for the $X\ ^1\Sigma^+$ state, we have predicted the location of the HF $v = 20$ vibrational level at an energy of $E_{20} = 49340.06\ cm^{-1}$, about $21.5\ cm^{-1}$ below the dissociation limit. The outer turning point is found at $R_{20}^+ = 3.86$ Å, which lies well into the long-range region, the onset of which is given by the Le Roy radius, $R = 3.12$ Å.[37] Although it may be tempting to calculate molecular constants for $v'' = 20$, and J-dependent Franck−Condon factors for prospective $v' - 20\ B \rightarrow X$ electronic emission bands, and to search carefully through the photographic plates of Di Lonardo and Douglas[36] to locate such bands, it is not expected that any such lines will be found. The maximum value of J in such bands is expected to be $J = 4$ to 5, and given the hot rotational distribution of the spectra, lines involving such low J values will, in practice, be far too weak to be found, despite possibly large Franck−Condon factors.

V. Conclusions

The present global analysis of spectroscopic data for the X and B states of HF and DF represents the most comprehensive investigation of these isotopologues to date. With the additional advantage that all radial functions are expressed in analytical form, the results will undoubtedly be of much significance in aiding future applications. The sets of calculated molecular constants for both electronic states not only succeed in representing the entire spectroscopic information to within the experimental errors but can also be used in performing extrapolations to higher J with greater reliability than with existing constants, which are obtained in the conventional way. The potential functions presented for both electronic states can be regarded as the best available functions of their type, and should aid in the evaluation of future ab initio studies.

Supporting Information Available: Molecular constants for all observed vibrational levels for both isotopologues and both electronic states. This material is available free of charge via the Internet at http://pubs.acs.org.

References and Notes

(1) Coxon, J. A.; Hajigeorgiou, P. G. *J. Mol. Spectrosc.* **1991**, *150*, 1.
(2) Coxon, J. A.; Hajigeorgiou, P. G. *J. Mol. Spectrosc.* **1990**, *142*, 254.
(3) Coxon, J. A.; Hajigeorgiou, P. G. *J. Mol. Spectrosc.* **1990**, *139*, 84.
(4) Coxon, J. A.; Hajigeorgiou, P. G. *J. Mol. Spectrosc.* **2000**, *203*, 49.
(5) Imes, E. S. *Astrophys. J.* **1919**, *50*, 251.
(6) Schaeffer, C.; Thomas, M. Z. *Phys.* **1923**, *12*, 330.
(7) Neufeld, D. A.; Zmuidzinas, J.; Schilke, P.; Phillips, T. G. *Astrophys. J. Lett.* **1997**, *488*, L141.
(8) Piecuch, P.; Kucharski, S. A.; Špirko, V. *J. Chem. Phys.* **1999**, *111*, 6679.
(9) Piecuch, P.; Kucharski, S. A.; Špirko, V.; Kowalski, K. *J. Chem. Phys.* **2001**, *115*, 5796.
(10) Li, X.; Paldus, J. *J. Chem. Phys.* **2002**, *117*, 1941.
(11) Martin, J. M. L. *Chem Phys. Lett.* **1998**, *292*, 411.
(12) Bettendorff, M.; Buenker, R. J.; Peyerimhoff, S. D.; Römelt, J. Z. *Phys. A* **1982**, *304*, 125.
(13) Douglas, A. E.; Greening, F. R. *Can. J. Phys.* **1979**, *57*, 1650.
(14) Coxon, J. A. *J. Mol. Spectrosc.* **1986**, *117*, 361.
(15) Kosman, W. M.; Hinze, J. *J. Mol. Spectrosc.* **1975**, *56*, 93.
(16) Vidal, C. R.; Scheingraber, H. *J. Mol. Spectrosc.* **1977**, *65*, 46.
(17) Hajigeorgiou, P. G.; Le Roy, R. J. *J. Chem. Phys.* **2000**, *112*, 3949.
(18) Coxon, J. A.; Hajigeorgiou, P. G. *J. Chem. Phys.* **2004**, *121*, 2992.
(19) Coxon, J. A.; Hajigeorgiou, P. G. *J. Mol. Spectrosc.* **1999**, *193*, 306.
(20) Coxon, J. A.; Dickinson, C. S. *J. Chem. Phys.* **2004**, *121*, 9378.
(21) Coxon, J. A.; Melville, T. C. *J. Mol. Spectrosc.* **2006**, *235*, 235.
(22) Le Roy, R. J. In *Molecular Spectroscopy, Specialist Periodical Report of the Chemical Society of London*; Barrow, R. F., Ed.; 1973; Vol. 1, Chapter 3.
(23) Gruebele, M. H. W.; Keim, E.; Stein, A.; Saykally, R. J. *J. Mol. Spectrosc.* **1988**, *131*, 343.
(24) Tiemann, E. *Mol. Phys.* **1988**, *65*, 359.
(25) Brühl, R.; Kapetanakis, J.; Zimmermann, D. *J. Chem. Phys.* **1991**, *94*, 5865.
(26) Hedderich, H. G.; Dulick, M.; Bernath, P. F. *J. Chem. Phys.* **1993**, *99*, 8363.
(27) White, J. B.; Dulick, M.; Bernath, P. F. *J. Chem. Phys.* **1993**, *99*, 8371.
(28) Campbell, J. M.; Dulick, M.; Klapstein, D.; White, J. B.; Bernath, P. F. *J. Chem. Phys.* **1993**, *99*, 8379.
(29) Watson, J. K. G. *J. Mol. Spectrosc.* **1980**, *80*, 411.
(30) Le Roy, R. J. *J. Mol. Spectrosc.* **1999**, *194*, 189.
(31) Herman, R. M.; Ogilvie, J. F. *Adv. Chem. Phys.* **1998**, *103*, 187.
(32) Ogilvie, J. F. *Proc. R. Soc. London, Ser. A* **1981**, *378*, 287.
(33) Le Roy, R. J.; Huang, Y. *J. Mol. Struct.: THEOCHEM* **2002**, *591*, 175.
(34) Mohr, P. J.; Taylor, B. N. *CODATA recommended values of the fundamental physical constants: 2002*; http://physics.nist.gov/lab.html.
(35) Audi, G.; Wapstra, A. H.; Thibault, C. *Nucl. Phys. A* **2003**, *729*, 337.
(36) Di Lonardo, G.; Douglas, A. E. *Can. J. Phys.* **1973**, *51*, 434.
(37) Coxon, J. A.; Hajigeorgiou, P. G. *J. Mol. Spectrosc.* **1989**, *133*, 45.
(38) Nolt, I. G.; Radostitz, J. V.; Di Lonardo, G.; Evenson, K. M.; Jennings, D. A.; Leopold, K. P.; Vanek, M. D.; Zink, L. R.; Chance, K. V. *J. Mol. Spectrosc.* **1987**, *125*, 274.
(39) Jennings, D. A.; Wells, J. S. *J. Mol. Spectrosc.* **1988**, *130*, 267.
(40) Odashima, H.; Zink, L. R.; Evenson, K. M. *J. Mol. Spectrosc.* **1999**, *194*, 283.
(41) Hedderich, H. G.; Frum, C. I.; Engleman, R.; Bernath, P. F. *Can. J. Chem.* **1991**, *69*, 1659.
(42) Ram, R. S.; Morbi, Z.; Guo, B.; Zhang, K.-Q.; Bernath, P. F.; Vander Auwera, J.; Johns, J. W. C.; Davies, S. P. *Astrophys. J., Suppl. Ser.* **1996**, *103*, 247.
(43) Lemoine, B.; Demuynck, C. Private communication, 1987.
(44) Sengupta, U. K.; Das, P. K.; Narahari Rao, K. *J. Mol. Spectrosc.* **1979**, *74*, 322.
(45) Deutsch, T. F. *Appl. Phys. Lett.* **1967**, *11*, 18.
(46) Mason, A. A.; Neilsen, A. H. *J. Opt. Soc. Am.* **1967**, *57*, 1464.
(47) Cuellar, E.; Pimentel, G. C. *J. Chem. Phys.* **1979**, *71*, 1385.
(48) Akitt, D. P.; Yardley, J. T. *J. Quantum Electron.* **1970**, *6*, 113.
(49) Rothschild, W. G. *J. Opt. Soc. Am.* **1964**, *54*, 20.
(50) Revich, V. E.; Stankevitch, S. A. *Dokl. Phys. Chem.* **1966**, *170*, 699.
(51) Goddon, D.; Groh, A.; Hanses, H. J.; Schneider, M.; Urban, W. *J. Mol. Spectrosc.* **1991**, *147*, 392.
(52) Le Blanc, R. B.; White, J. B.; Bernath, P. F. *J. Mol. Spectrosc.* **1994**, *164*, 574.
(53) Guelachvili, G. *Opt. Commun.* **1976**, *19*, 150.

(54) Webb, D. U.; Narahari Rao, K. *J. Mol. Spectrosc.* **1968**, *28*, 121.

(55) Herget, W. F.; Deeds, W. E.; Gailar, N. M.; Lovell, R. J.; Nielsen, A. H. *J. Opt. Soc. Am.* **1962**, *52*, 1113.

(56) Mann, D. E.; Thrush, B. A.; Lide, D. R., Jr.; Ball, J. J.; Acquista, N. *J. Chem. Phys.* **1961**, *34*, 420.

(57) Deutsch, T. F. *Appl. Phys. Lett* **1967**, *10*, 234.

(58) Sasada, H. *J. Mol. Spectrosc.* **1994**, *165*, 588.

(59) Fishburne, E. S.; Rao, K. N. *J. Mol. Spectrosc.* **1966**, *19*, 290.

(60) De Lucia, F. C.; Helminger, P.; Gordy, W. *Phys. Rev A* **1971**, *3*, 1849.

(61) Hajigeorgiou, P. G. Ph.D. Thesis, Dalhousie University, 1991.

(62) Spanbauer, R. N.; Narahari Rao, K.; Jones, L. H. *J. Mol. Spectrosc.* **1965**, *16*, 100.

(63) Zemke, W. T.; Stwalley, W. C.; Coxon, J. A.; Hajigeorgiou, P. G. *Chem. Phys. Lett.* **1991**, *177*, 412.

(64) Hu, Q. J.; Hepburn, J. W. *J. Phys: Conf. Proc.* **2005**, *4*, 267.

(65) Dunham, J. L. *Phys. Rev.* **1932**, *41*, 721.

(66) Hajigeorgiou, P. G. *J. Mol. Spectrosc.* **2006**, *235*, 111.

(67) Hutson, J. M. *J. Phys. B* **1981**, *14*, 851.